

Wetland Accretion Rate Model of Ecosystem Resilience (WARMER) and Its Application to Habitat Sustainability for Endangered Species in the San Francisco Estuary

Kathleen M. Swanson · Judith Z. Drexler · David H. Schoellhamer ·
Karen M. Thorne · Mike L. Casazza · Cory T. Overton ·
John C. Callaway · John Y. Takekawa

Received: 19 April 2012 / Revised: 11 July 2013 / Accepted: 2 August 2013 / Published online: 25 September 2013
© Coastal and Estuarine Research Federation (outside the USA) 2013

Abstract Salt marsh faunas are constrained by specific habitat requirements for marsh elevation relative to sea level and tidal range. As sea level rises, changes in relative elevation of the marsh plain will have differing impacts on the availability of habitat for marsh obligate species. The Wetland Accretion Rate Model for Ecosystem Resilience (WARMER) is a 1-D model of elevation that incorporates both biological and physical processes of vertical marsh accretion. Here, we use WARMER to evaluate changes in marsh surface elevation and the impact of these elevation changes on marsh habitat for specific species of concern. Model results were compared to elevation-based habitat criteria developed for marsh vegetation, the endangered California clapper rail (*Rallus longirostris obsoletus*), and the endangered salt marsh harvest mouse (*Reithrodontomys raviventris*) to determine the response of marsh habitat for each

species to predicted >1-m sea-level rise by 2100. Feedback between vertical accretion mechanisms and elevation reduced the effect of initial elevation in the modeled scenarios. Elevation decreased nonlinearly with larger changes in elevation during the latter half of the century when the rate of sea-level rise increased. Model scenarios indicated that changes in elevation will degrade habitat quality within salt marshes in the San Francisco Estuary, and degradation will accelerate in the latter half of the century as the rate of sea-level rise accelerates. A sensitivity analysis of the model results showed that inorganic sediment accumulation and the rate of sea-level rise had the greatest influence over salt marsh sustainability.

Keywords Accretion · Endangered species · Habitat sustainability · Numerical model · Salt marsh · San Francisco Estuary · Sea-level rise

Communicated by Carolyn A. Currin

Electronic supplementary material The online version of this article (doi:10.1007/s12237-013-9694-0) contains supplementary material, which is available to authorized users.

K. M. Swanson (✉) · J. Z. Drexler · D. H. Schoellhamer
U.S. Geological Survey, California Water Science Center,
6000 J Street, Placer Hall, Sacramento, CA 95819-6129, USA
e-mail: kathleen.swanson@gmail.com

K. M. Thorne · J. Y. Takekawa
U.S. Geological Survey, Western Ecological Research Center, San
Francisco Bay Estuary Field Station, 505 Azuar Drive,
Vallejo, CA 94592, USA

M. L. Casazza · C. T. Overton
U.S. Geological Survey, Western Ecological Research Center, Dixon
Field Station, 69924 Tremont Rd., Dixon, CA 95620, USA

J. C. Callaway
University of San Francisco,
Department of Environmental Science, 2130 Fulton St.,
San Francisco, CA 94117, USA

Introduction

Rising sea levels over the next century and beyond are a threat to the sustainability of tidal marshes in coastal regions throughout the world (Hatton et al., 1983; Nicholls et al. 1999; FitzGerald et al., 2008). While some tidal marshes may be able to keep pace with various scenarios of sea-level rise (SLR), changes in elevation relative to mean sea level (MSL) may alter basic habitat characteristics such as inundation frequency, inundation duration, and salinity (Day and Templet, 1989; Erwin et al., 2006; Takekawa et al., 2013). Such changes may ultimately impact the quality and accessibility of marsh habitat, thus impacting the critical habitat for endemic salt marsh obligates.

The relative elevation of the marsh plain increases with inorganic sediment deposition and organic matter accumulation and decreases with eustatic SLR, decomposition of

organic material, and compaction of deposited soils (Allen, 1995; Callaway et al., 1996; Day et al., 1999; Morris et al., 2002; D'Alpaos et al., 2007; Kirwan and Murray, 2007; Drexler et al., 2009; Drexler, 2011). Relative elevation is inversely related to inundation time and the corresponding sediment flux at a given elevation. Decreasing sediment accumulation at increasing elevations should create a negative or stabilizing feedback that allows marshes to maintain an equilibrium elevation (Krone, 1987). Maintenance of marsh elevation during periods of subsidence and accelerated SLR is critical for the survival of species that are adapted to the tidal inundation regime of a marsh.

Simulations of tidal marsh vertical accretion are useful tools for exploring the potential impacts of SLR on salt marsh elevation. Such numerical models have been used to predict elevation changes within salt marshes for scenarios of SLR, changes in sediment input, and other environmental forcings (French, 1993; Allen, 1995; Callaway et al., 1996; Morris et al., 2002; French, 2006; Kirwan and Murray, 2007; D'Alpaos, 2011). Krone (1987) modeled the impact of SLR on historic marsh and mudflat elevations in the San Francisco Estuary by predicting the settling flux of suspended sediment with a simple 0-D model and concluded that despite the stabilizing feedback between elevation and sediment accumulation, relative salt marsh elevation will only remain constant if the rate of SLR is stable.

In contrast to Krone (1987), French (1993) incorporated the accumulation of organic material and autocompaction as well as relative SLR and mineral sediment accumulation in a 1-D (vertical) model of marsh elevation. The model predicted “drowning” of salt marsh habitats in the near-future, under scenarios of what were then considered extreme accelerations in relative SLR, and survival with some decrease in elevation for more moderate scenarios. French (1993) noted that either of these scenarios would impact the inundation regime and habitat functionality even if the marsh vegetation and morphology were maintained with only small changes in relative elevation during a period of accelerated SLR. Other models of vertical marsh accretion incorporate decay of organic material (Callaway et al., 1996; Day et al., 1999; Rybczyk and Cahoon, 2002; Kirwan and Murray, 2007; Mudd et al., 2009) and feedback between inundation regime (elevation) and organic matter production (Morris et al., 2002). Cahoon et al. (1995) found that vertical accretion alone was not an adequate surrogate for elevation change because of the importance of belowground processes. Morris et al. (2002) improved upon previously modeled organic matter accumulation by fitting a parabolic curve to productivity of the salt marsh cordgrass (*Spartina alterniflora*) found along the Atlantic coast of the USA. The dynamic feedback between elevation and organic matter accumulation is vital to accurately predicting marsh response to SLR (French, 2006; Kirwan and Murray, 2007; Kirwan et al., 2009; Kirwan and Guntenspergen, 2012). In sediment-limited marshes, high organic matter

accumulation can outpace inorganic sediment accumulation and account for more elevation per mass than inorganic sediment because of the low particle density of organic matter (Bricker-Urso et al., 1989; Kirwan and Murray, 2007; Drexler, 2011).

The marsh accretion model presented in this study is an adaptation of the Fortran model developed by Callaway et al. (1996), hereafter the Callaway model. The Callaway model calculates changes in elevation relative to MSL of a unit area representative of the marsh surface based on changes in relative sea level, subsidence, inorganic sediment accumulation, aboveground and belowground productivity, compaction, and decay. The Callaway model includes a constant rate of SLR, a constant organic matter input rate, and a linear relationship between elevation and inorganic matter accumulation based on French (1993). Organic matter inputs are divided between above- and belowground components, and belowground organic matter is distributed such that the mass of new organic matter per cohort decreases exponentially with increasing depth in the soil column. The rate of decomposition of organic matter is a function of both depth and age of the organic matter. Compaction is a function of the mass above a given cohort and the porosity at depth within the soil column.

The Callaway model has previously been applied to project vertical accretion rates in impounded freshwater marshes in the Sacramento–San Joaquin Delta of California (Deverel et al., 2008). Here, we use an adaptation of the Callaway model to evaluate scenarios of marsh elevation change in salt marshes in the San Francisco Estuary for scenarios of temporally variable SLR and elevation-dependent inorganic and organic matter inputs. The resilience of tidal marsh habitats is of particular interest in the San Francisco Estuary, where sea level and other climate-driven changes are expected to be significant over the twenty-first century (Cloern et al. 2011).

San Francisco Estuary tidal marsh habitat supports both the federally endangered *Reithrodontomys raviventris* and *Rallus longirostris obsoletus*. Up to 95 % of historic marshes in San Francisco Estuary have been lost in the past two centuries, resulting in highly fragmented wetland habitats within the estuary that provide critical habitat for these species (Mitsch and Gosselink, 2000; Euliss et al., 2008; California State Coastal Conservancy, 2010). These species inhabit, feed, and breed within marshes where even slight changes to marsh elevation can dramatically decrease the effective habitat during high tides when the marsh plain is inundated. Such changes in elevation relative to MSL would likely have negative impacts on *R. raviventris* and *R. longirostris obsoletus* due to increases in predation, a reduction of the area of marsh that produces food for each species, and nest failure and mortality due to increased frequency and depth of tidal flooding (Van de Pol et al., 2010; Takekawa et al., 2013).

The objectives of this study were to (1) simulate scenarios of salt marsh accretion as sea level rises, (2) evaluate the

evolution of the marsh surface elevation as a result of SLR, and (3) evaluate the long-term sustainability of salt marsh habitat for *R. raviventris* and *R. longirostris obsoletus*.

Methods

Field Sites and Habitat Evaluation

The model developed here was applied to four salt marshes in San Francisco Estuary: Coon Island, a portion of Petaluma marsh, China Camp marsh, and Laumeister marsh (Fig. 1; Table 1). These marshes have high marsh

platforms fringed by cordgrass (*Spartina* spp.) and dominated by common pickleweed (*Sarcocornia pacifica*) (Takekawa et al., 2013). Coon Island is a salt marsh on the Napa River. Petaluma marsh is part of the largest undisturbed salt marsh in the estuary and is located on the Petaluma River. China Camp marsh is located in China Camp State Park in San Pablo Estuary. Laumeister marsh is located in South San Francisco Bay. Tidal range varies from 140 to 169 cm between sites as do absolute elevation (typically about mean high water (MHW)) and accretion rate (Takekawa et al., 2013; Callaway et al., 2012). The area, latitude, and longitude of each field site are provided in Table 1.

Fig. 1 Aerial view of the San Francisco Estuary and field sites: 1 Coon Island marsh, 2 Petaluma River marsh, 3 China Camp marsh, and 4 Laumeister marsh

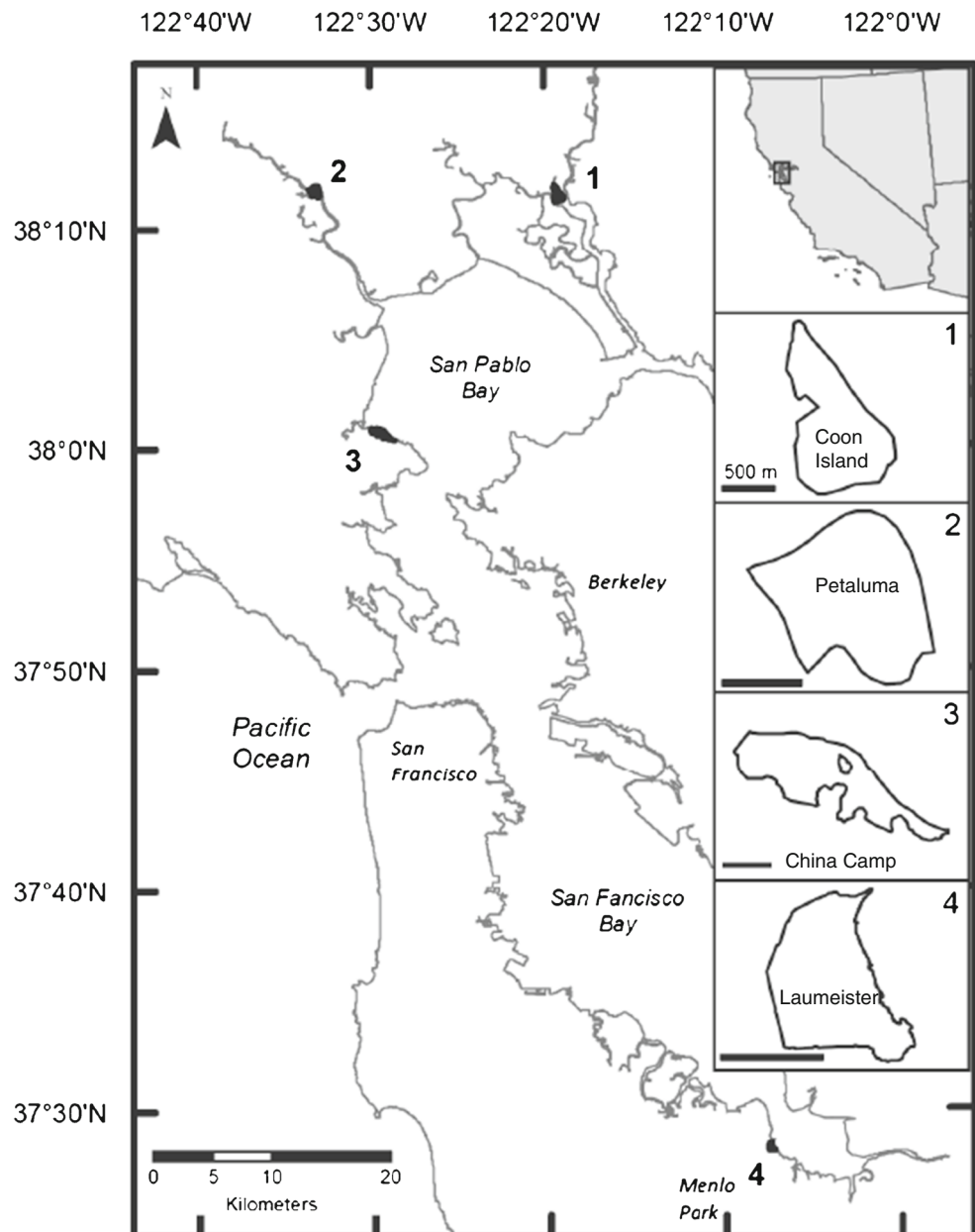


Table 1 Location of each field site, measured marsh area, and the number of topographic survey points and vegetation quadrats measured at each site. Only a portion of the large Petaluma River marsh was surveyed and included in this project

	Latitude	Longitude	Area (hectares)	Survey points	Quadrats measured	Tide range (cm)
Coon Island	38°11'33" N	122°18'59" W	98.7	799	364	143
Petaluma	38°11'40" N	122°33'08" W	80.6	655	357	143
China Camp	38°00'45" N	122°29'35" W	96.6	754	409	140
Laumeister	37°28'17" N	122°07'30" W	36.8	717	72	169

Marsh Topography and Hydrology

Field site elevations were surveyed with a Leica RX1200 Real Time Kinematic Global Positioning System rover (± 3 cm x , y , z accuracy; Leica Geosystems Inc., Norcross, GA, USA) once at each site between 2009 and 2010 in conjunction with percent plant cover and plant height measurements by species at approximately one half of all survey points (Takekawa et al., 2013). The number of survey points and 0.25-m² vegetation quadrats that were measured within each site are provided in Table 1. Topographic survey data were used to develop a digital elevation map (DEM) of each field site with 30-m grid spacing. Water depths on the marsh plain and in adjacent channels were also recorded with a Solonist 3001 levellogger Junior with an accuracy of 0.1 % (a maximum error of ± 1 cm) every 6 min for a period of 12 months at each site in order to establish local inundation regimes. Mean sea level at each site was determined from the interpolated sea surface topography available in the National Oceanic and Atmospheric Administration VDatum database of regional tidal datums for the San Francisco Bay area (Xu et al., 2010). The maximum cumulative error associated with the tidal datums in this database is 9.8 cm, and the error associated with conversion between MSL and the North American Vertical Datum of 1988 (NAVD 88) is 0.1 cm. Marsh surface elevation, water level, and vegetation data are reported in detail in Takekawa et al. (2013). Because the hydrology and inundation of the marsh plain are not directly comparable to the adjacent open water for which tidal datums were developed, site-specific datums of MHW, mean higher high water (MHHW), and maximum annual tide height (MAT) were determined with measured inundation from the sensors on the marsh plain.

Elevation data are reported as (1) absolute elevation relative to the North American Vertical Datum 1988 (NAVD88), (2) elevation relative to local MSL, or (3) a dimensionless elevation relative to the tidal range of the site. This third measure was chosen to facilitate comparison between sites, which would otherwise be confounded by the variability of MSL and tidal range between sites. The relative elevation within the tidal frame, z^* , is the dimensionless number that reflects the elevation relative to R , which is calculated as

$$R = MHHW - MSL \quad (1)$$

and z^* is the dimensionless ratio of the elevation relative to MSL, z -MSL, and R

$$z^* = \frac{z - MSL}{R} \quad (2)$$

Tidal datums, elevations, and R have units of length, $[L]$. By definition, $z^*=0$ at MSL and $z^*=1.0$ at MHHW. Tidal datums and corresponding z^* values are reported in Table 2.

WARMER

The Wetland Accretion Rate Model of Ecosystem Resilience (WARMER) is a 1-D cohort model of wetland accretion based on the Callaway et al. (1996) model (Fig. 2). Each modeled cohort is the mass of inorganic and organic matter accumulated at the surface in a single year with any subsequent below-ground organic matter productivity (root growth) less decay. Cohort density, a function of mineral, organic, and water content, is calculated at each time step to account for decay of organic material and autocompaction of the soil column. The change in relative elevation is then equal to the difference between the change in sea level and the change in height of the soil column, which is the sum of the volume of all cohorts over the unit area model domain. Each of these inputs and any changes to them are discussed in more detail below.

WARMER expands upon the Callaway model by including (1) the feedback between organic matter accumulation and elevation, (2) a nonlinear relationship between inorganic matter accumulation and elevation, and (3) a temporally variable SLR. While other models have incorporated these three improvements in various combinations, the adaptation of the Callaway model to include these provides a computationally efficient 1-D model that should capture the dynamics of critical accretion processes in salt marshes, with input functions defined specifically for the San Francisco Estuary or individual sites. The elevation computed in WARMER of the marsh surface, E $[L]$, at time t relative to local MSL is

$$E(t) = E(0) - SLR(t) + \sum_{i=0}^t V_i(t) \quad (3)$$

Table 2 Water surface elevations for critical tidal datums: maximum annual tide (MAT), mean higher high water (MHHW), mean high water (MHW), mean sea level (MSL), mean low water (MLW), and mean

lower low water (MLLW). Data are reported in meters (NAVD88 and dimensionless elevation relative to local mean sea level, z^* , as defined in Eq. 3

	MAT		MHHW		MHW		MSL		MLW		MLLW	
	(m)	z^*	(m)	z^*	(m)	z^*	(m)	z^*	(m)	z^*	(m)	z^*
China Camp	2.46	1.54	1.95	1	1.77	0.81	1.01	0	0.37	-0.68	0.06	-1.01
Petaluma	2.36	1.52	1.92	1	1.76	0.82	1.06	0	0.33	-0.85	0.07	-1.15
Coon Island	2.37	1.5	1.94	1	1.78	0.81	1.07	0	0.35	-0.83	0.09	-1.14
Laumeister	2.71	1.69	2.09	1	1.92	0.81	1.18	0	0.23	-1.05	-0.02	-1.32

where $E(0)$ is the initial elevation relative to MSL, $SLR(t)$ is the sea level at time t relative to the initial sea level, and $V_i(t)$ is the volume per unit area, or height, at time t of the cohort formed during year i . The total volume of an individual cohort is the sum of the mass of water, calculated from the porosity of the cohort, mineral sediment, and organic matter divided by the cohort bulk density.

Local SLR

The magnitude of response of marsh accretion and elevation to SLR varies as a function of elevation relative to local sea

level. The timing and rate of SLR are required inputs to assess the response of marshes to SLR rather than just the mean rate of change over the time period of interest. WARMER incorporates a recent forecast of SLR for the San Francisco Estuary (Cayan et al., 2009) based on a moderate emissions scenario (A2 in IPCC Fourth Assessment Report, Bindoff et al., 2007). This SLR prediction based on the mean SLR produced by the A2 group of scenarios has been adapted to San Francisco Estuary and forecasts a 124-cm increase in sea level from 2000 to 2100 (Fig. 3). WARMER assumes that the tide range remains constant in time and only the mean sea level changes annually.

Inorganic Sediment Input

The Callaway model includes a mineral sediment input function based on French (1993), where sediment deposition increases linearly with decreasing depth from MAT to MSL and is constant below MSL. While this function is a

Conceptual Model

Relative sea-level rise



Above ground productivity



Sediment input



Root growth



Compaction



Decay



Cohort based model with an annual timestep

Fig. 2 Model schematic showing the inputs to WARMER. Arrows indicate where there is a given process that increases (right) or decreases (left) the relative elevation of the marsh surface

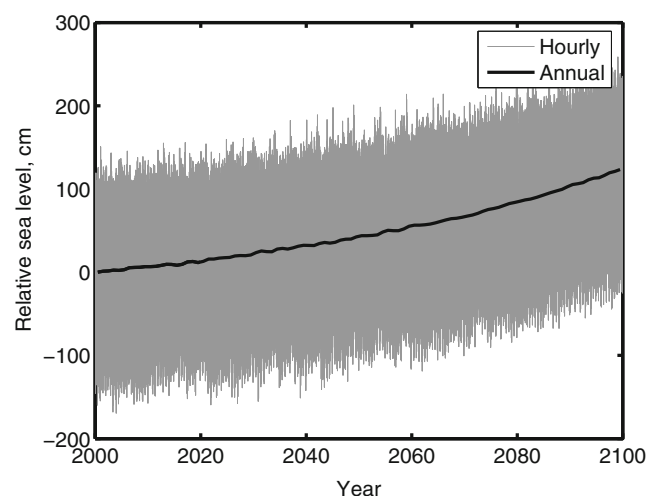


Fig. 3 Hourly relative water level prediction from Cayan (Cayan et al., 2009) and 1-year running mean of hourly data. The average annual SLR curve was used as the input function for the model with a net change of 124 cm from 2000 to 2100

good approximation above MSL for a system with sinusoidal tides and constant suspended-sediment concentrations, the inundation frequency of each marsh in this study has been measured and can be described more precisely for the mixed semi-diurnal tides in San Francisco Bay. Sediment concentration varies over tidal, seasonal, and annual timescales (Schoellhamer, 2002). The tidal time-scale controls the relative strength of the negative feedback between elevation and sediment accumulation that is critical to maintaining marsh elevation. Schoellhamer (1996) demonstrated that sediment concentrations in South San Francisco Bay are higher in shallow water less than 2 m deep than in the deeper channels, and Ruhl and Schoellhamer (2004) demonstrated that the shallow mudflats act as a temporary storage for estuarine sediments. It is likely that sediment stored in shallow mudflats is reworked on rising and falling tides and the highest concentrations at the bay edge occur out of phase with the highest concentrations in the channels. There is insufficient monitoring data at the edges of the estuary or within marshes to properly parameterize the effect of the temporal variability of sediment supply on tidal timescales. Therefore, like Callaway et al. (1996), French (1993), and Stralberg et al. (2011), the simplifying assumption of a constant sediment concentration was used. This approach assumes that vegetation does not increase the amount of sediment deposited on the marsh surface. Sediment flux from the water column to the marsh surface at a given elevation, z , is assumed equal to the product of suspended-solid concentration (SSC) and settling velocity summed over all times that elevation z is inundated. For the case of constant SSC and settling velocity, the mass accumulation is directly proportional to the inundation frequency and can be calibrated from measured accumulation rates without any direct measurement of concentration or settling velocity. This sediment flux at a given elevation, z , measured in mass per unit area per year $[\frac{M}{L^2T}]$, $M_s(z)$, is equal to

$$M_s(z) = S^* f(z) \quad (4)$$

where $f(z)$ is the dimensionless inundation frequency as a function of elevation and $S [\frac{M}{L^2} \cdot \frac{L}{T}]$ is the maximum potential sediment flux determined by calibration to sediment accumulation data.

Sediment cores collected and analyzed to determine the vertical profiles of ^{210}Pb and ^{137}Cs (Callaway et al., 2012) were used to calibrate the sediment accumulation function described above. Accretion rates were determined at each site except for Laumeister marsh where the data sets of Takekawa et al. (2013) and Callaway et al. (2012) did not overlap. Accretion rates for Whale's Tail, which is situated

in close proximity to Laumeister marsh and has very similar plant community composition, were used for Laumeister marsh accretion. A subset of post-1963 mineral and organic matter accumulation rates for cores, in which the 1963 sediment horizon identified by ^{210}Pb dating was also verified by the ^{137}Cs dating, was used as model inputs. Whale's Tail accumulation rates could only be determined using the ^{137}Cs dating. The sediment accumulation curve described in Eq. 4 was then fit to the measured accumulation rates using a least squares method.

Schoellhamer (2011) indicates that a step decrease in suspended-sediment concentration in the estuary occurred beginning in 1999. The limited data set of marsh cores was insufficient to observe a corresponding change in inorganic sediment accumulation. Thus, the inorganic sediment accumulation rate since 1963 was used to calibrate the sediment input function (Fig. 4a).

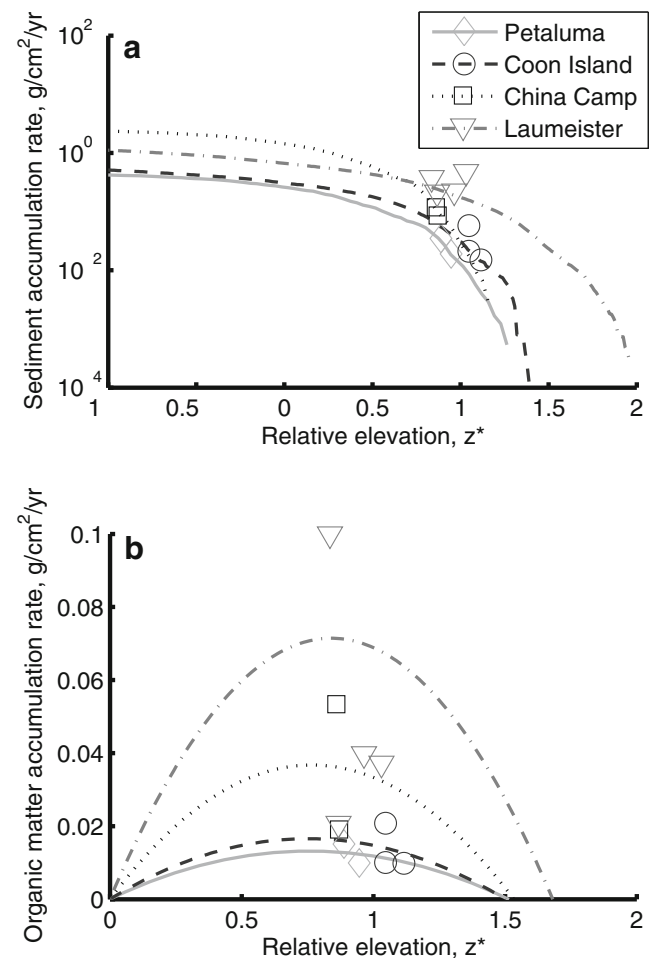


Fig. 4 Calculated sediment accumulation curves (lines) and measured accumulation rates (points) for all four salt marsh sites plotted as a function of dimensionless elevation, z^* (a), and calculated organic matter accumulation (lines) and measured accumulation rates (points) in each marsh plotted as a function of dimensionless elevation (b)

Above- and Belowground Organic Matter Inputs

The salt marshes in the San Francisco Estuary selected for this study are dominated by *S. pacifica*, with a *Spartina foliosa* fringe at low elevation. Because little is known about the elevation-productivity feedback function at the other study sites, the productivity function developed by Morris et al. (2002) for *S. alterniflora* was adapted to the elevation range of vegetation and measured organic matter accumulation in the selected sites. The shape of the curve that Morris et al. (2002) developed for *S. alterniflora* salt marshes, which has been confirmed as the general shape of productivity for *Schoenoplectus americanus* and *Spartina patens* by Kirwan and Guntenspergen (2012), was retained here, but the elevation range of vegetation, the roots of the parabolic equation, and the magnitude of organic matter input were adjusted for San Francisco Estuary marsh vegetation (Fig. 4b). Vegetation cover is roughly parabolic between MSL and MAT (Fig. 5), with a tailing fringe of *S. foliosa* cover (<35 %) below MSL, but very little marsh area extends below MSL (<1 %). Hence, the roots of the parabolic function were fixed at MSL and MAT for each site, and the magnitude was calibrated to the measured organic matter input rates from the sediment cores. The parabolic equation describing the annual mass of organic matter accumulated per unit area [$\frac{M}{L^2T}$], M_o at elevation z is then

$$M_o(z) = (a + b)(z - MSL)(z - MAT) \tag{5}$$

where a and b are constants with units of [$\frac{M}{L^2T}$] for above- and belowground organic matter accumulations, respectively, fit to the measured organic matter accumulation rates in the surface layer of each sediment core for each marsh at specified elevations. The organic matter accumulation rate was determined from the mineral sediment accumulation rate and the ratio of

sediment to organic material in the surface layer of each sediment core. Though the organic matter accumulation may be slightly underestimated because some decay will occur prior to core collection, this bias is minimized by also calculating key decay parameters from this same data as discussed below. Although additional feedback between elevation and productivity may enhance root growth across several species in mid-Atlantic salt marshes (Kirwan and Guntenspergen, 2012), the relationships between above- and belowground productivity and elevation for *S. pacifica* or other Pacific marsh species have not been well constrained, and therefore, they are not included here. For the purposes of this paper, organic matter input is divided between above- and belowground inputs using a shoot-to-root ratio of $a/b = 0.57$ based on the work of Scarton et al. (2002) and Curc3o et al. (2002) for *Sarcocornia*. The mass of the organic material generated below ground each year is distributed exponentially with depth, and the coefficient of exponential decay, k_{dist} , is set equal to 1.0 (Deverel et al., 2008).

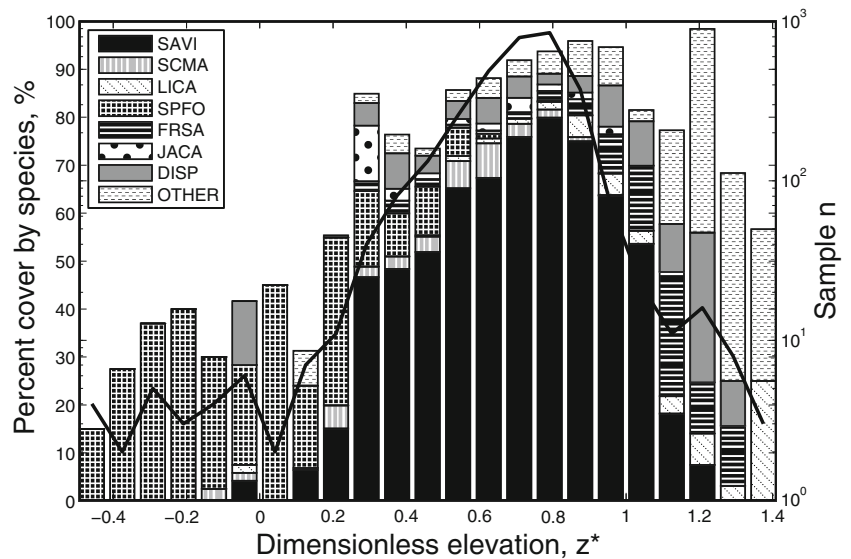
Compaction and Decomposition

Compaction and decomposition functions of WARMER follow the Callaway model. Compaction of highly porous marsh soil is determined by a rate of decrease in porosity from the average measured porosity of the top 5 cm of each sediment core and a lower limit of porosity measured at the bottom 5 cm of each sediment core. The rate of decrease, r , in porosity of a given cohort is a function of the density of all of the material above that cohort such that

$$r = 1 - \frac{\rho_b}{k_1 - \rho_b} \tag{6}$$

where ρ_b is the density of the material above a cohort and k_1 is a calibration constant from Deverel et al. (2008).

Fig. 5 Vegetation cover by plant species as a function of dimensionless elevation, z^* . The number of samples, n , at each elevation interval is plotted on the right-hand log-scale y -axis. Legend entries refer to plant species: SAVI is *S. pacifica*, SCMA is *Scirpus maritimus*, LICA is *Limonium californicum*, SPFO is *S. foliosa*, FRSA is *Frankenia salina*, JACA is *Jaumea carnosa*, and DISP is *Distichlis spicata*



Decomposition is assumed to follow a three-stage process where the youngest organic material less than 1 year old decomposes at the fastest rate, the organic matter 1 to 2 years old decays at a moderate rate, and the organic matter greater than 2 years old decays at the slowest rate. The percentage of refractory organic material is determined by dividing the mean percent organic matter at the top of a core by the mean percent organic matter in the bottom 4 cm of the core. The fraction of nonrefractory organic material, F_{Mo} , in each age class remaining after each time step is calculated as

$$F_{Mo}(i, d) = C(i)\exp(-k_{decomp}(i)\cdot d) \quad (7)$$

where d is the depth of the cohort and coefficients $C(i)$ and $k_{decomp}(i)$ are coefficients for each age class, i , and are determined empirically by measuring the remaining mass of organic material in decomposition bags at varying times after initial placement. For this study, we used values for *Typha* spp., *Schoenoplectus* spp., and *Phragmites australis* under similar climates compiled by Deverel et al. (2008).

Model Application

The 1-D model was applied at three elevations (low, mean, and high) for each site, and the results were interpolated across the marsh surface to determine changes in area of effective habitat. Mean, low, and high elevations were calculated from the measured mean elevation from the marsh DEM, \bar{z} , and the mean ± 2 standard deviations from the mean elevation of the marsh surface, $\bar{z} \pm 2\sigma$. For any point on the marsh surface with a starting elevation, z , between the high and low initial elevations modeled, $\bar{z} + 2\sigma > z > \bar{z} - 2\sigma$, the projected marsh surface elevations were calculated as the distance-weighted average of the two model simulations with the closest initial elevations. The results from the nearest initial elevation were applied without any weighting to any initial elevations on the marsh plain outside of this range.

The model calculated changes to the mass and volume of annual cohorts of sediment and organic matter on a 1/10-year time step for a total run of 100 years, 2000–2099. A spin-up time of 200 years with a constant rate of SLR required to maintain the desired initial elevation was used for all scenarios to establish a sediment column that represented the existing marsh. The model results were calculated for the four salt marsh sites, and the potential impact of elevation changes on the effective habitat of *R. raviventris* and *R. longirostris obsoletus* was evaluated. The input parameters required to run the model are shown in Table 3.

Model Performance Test

Marsh vertical accretion data for a site are seemingly always scant such that independent calibration and validation data

sets are not available. Callaway et al. (1996) compare vertical accretion of modeled marsh surfaces to the ^{137}Cs determined accretion rate measured in sediment cores that were also used to parameterize model inputs. Deverel et al. (2008) validated the adaptation of the Callaway et al. (1996) model to managed marshes by comparing the modeled and measured elevation changes for a 12-year simulation period. Corresponding measurements of accumulation and bulk density were used to parameterize the scenarios, and the validation primarily served as a test of decomposition and compaction algorithms (Deverel et al., 2008).

As a test of model performance in this study, we compared current marsh elevations and vegetation with computed equilibrium elevations. SLR was a constant equal to the long-term SLR trend of 2.1 mm/year at the mouth of San Francisco Bay from 1897 to 2006 (Zervas, 2009). The soil profiles for percent organic matter and bulk density generated from 200 years of 2.1-mm/year SLR were compared to soil core profiles at the sites, and computed equilibrium elevations and colonization elevations of San Francisco Estuary marsh vegetation (Atwater and Hedel, 1976) were compared to existing vegetation elevations. We also compared the SLR required to maintain the present elevations for the 12 model scenarios during the 200-year spin-up period to measured SLR. These comparisons do not constitute a true model validation, but data availability limits the ability to conduct a more rigorous validation. Stralberg et al. (2011) note the opportunity for future marsh monitoring to serve as a validation of marsh elevation projections.

Sensitivity Analysis

WARMER was run for a range of values of sediment input, organic matter input, SLR, and initial elevation in order to explore the model sensitivity within the described parameter space. The values were chosen to reflect the expected and extreme values of sediment and organic matter accumulation, porosity, SLR, and initial marsh elevation that have been measured or are anticipated in the San Francisco Estuary (Callaway et al., 2012). The initial elevation range and tide range of China Camp marsh were used to parameterize the model. The ranges of values for sediment accumulation, organic matter accumulation, and porosity were determined from the mean, minimum, and maximum values from all sites. Low and high estimates of the magnitude of SLR over the next century, 50 and 150 cm, respectively, by the California Climate Change Center (Cayan et al. 2009) were used in the sensitivity analysis. These parameters (Table 4) allowed for 243 simulations of marsh elevation.

Habitat Evaluation

Evaluation of habitat resilience was defined by (1) inundation tolerance of dominant vegetation and (2) availability of

Table 3 Model input parameters for all sites. Sediment accumulation rate is reported at the elevation of MSL. The organic matter accumulation curve calibration constants (*a* and *b*) have units of milligrams per quartic

centimeter per year which, when substituted in Eq. 5, yield an organic mass accumulation rate with units of milligrams per square centimeter per year

	Sediment $M_s(\text{MSL})$ (g/cm ² /year)	Organic matter		Porosity		Decay		Elevation	
		<i>a</i> (mg/cm ⁴ /year)	<i>b</i> (mg/cm ⁴ /year)	Surface (%)	Depth (%)	Refractory C (%)	$z-2\sigma$ (cm)	<i>z</i> (cm)	$z+2\sigma$ (cm)
China Camp	0.32	-2.57E-03	-4.52E-03	82	77	12	64	77	90
Petaluma	0.1	-1.13E-03	-1.99E-03	83	80	14	65	77	89
Coon Island	0.59	-1.42E-03	-2.50E-03	83	78	55	49	75	101
Laumeister	1.35	-4.43E-03	-7.77E-03	73	63	39	69	83	96

effective marsh habitat for cover, feeding, and reproduction for both *R. raviventris* and the *R. longirostris obsoletus* (Table 5). An explanation of each of the habitat metrics used and how they were determined is provided below.

Vegetation

In the San Francisco Estuary, the dominant low marsh vegetation is cordgrass (*Spartina* spp.) with the upper marshes dominated by pickleweed (*S. pacifica*). *S. alterniflora* was introduced to the Bay in 1973 (Faber, 2000), and it has since hybridized extensively and spread to a larger elevation range than the native *S. foliosa*. As of 2010, 34 ha of invasive *Spartina* was inventoried in the estuary, and small areas (order [10–100] m²) of *S. alterniflora* hybrids were found in or near China Camp, Petaluma, and Laumeister marshes (Hogle and Olofson, 2011). There is an on-going effort to eradicate *S. alterniflora* and its hybrids through physical removal and chemical treatments, but it is unclear whether total eradication will be possible (Hogle and Olofson, 2011). Data collected by Takekawa et al. (2013) at 13 tidal marshes in San Francisco Estuary, including the four salt marshes in this study, indicate that the transitional elevation from mudflat to *Spartina* spp. occurs below $z^*=0$ and the transition from *Spartina* spp. to *S. pacifica* occurs at approximately $z^*=0.3$ (Fig. 5). Projected changes in the relative areas of marsh habitat above and below these datums were used to assess the projected effective range for *Spartina* spp. and *S. pacifica*.

R. Raviventris

The decrease of salt marsh area and fragmentation has led to the designation of the salt marsh harvest mouse, *R. raviventris*, as an endangered species in the 1970s by the U.S. Fish and Wildlife Service and the California Department of Fish and Game (Federal Register 35: 16047). *R. raviventris* is an endemic small mammal whose life history is closely tied to the salt marsh landscape (Shellhammer, 1982). The mouse is well adapted to its environment and prefers areas dominated by dense stands of *S. pacifica* above MHHW. These areas are used for feeding and nesting sites, and protection from predation (Fisler, 1963, 1965; Shellhammer, 1982, Bias and Morrison, 2006). *R. raviventris* has been shown to move out of dense *S. pacifica* vegetation only during extreme high water events (Shellhammer, 1982; Bias and Morrison, 1999; Hulst et al., 2001) at which time they are vulnerable to drowning and predation. The presence of *S. pacifica*, located above MHHW, provides the necessary habitat and refuge for *R. raviventris*, and for this study, the area of marsh above MHHW ($z^*>1$) was used to evaluate the availability of effective habitat for the mouse.

R. Longirostris Obsoletus

The California clapper rail, *R. longirostris obsoletus*, is an endemic foraging bird found only within the tidal marshes of the San Francisco Estuary. *R. longirostris obsoletus* seeks refuge and nests within the emergent marsh vegetation and

Table 4 High, mean, and low parameter values used in the sensitivity analysis

	Sediment $M_s(\text{MSL})$ (g/cm ² /year)	Organic matter		Porosity		Elevation
		<i>a</i> (mg/cm ⁴ /year)	<i>b</i> (mg/cm ⁴ /year)	Surface (%)	Depth (%)	<i>z</i> (cm)
Low	0.32	-0.00113	-1.99E-03	78	77	64
Mean	0.77	-0.00238	-4.17E-03	81.5	78	77
High	2.23	-0.00769	-7.69E-03	83	80	90

Table 5 Elevation criteria used to evaluate suitable habitat area for each species of interest. Multiple habitat metrics are used for vegetation type and clapper rail habitat use

	Evaluation criteria	Explanation
Vegetation	% area where $z^* > 0.3$	Pickleweed (<i>S. pacifica</i>) habitat
	% area where $0 < z^* < 0.3$	Cordgrass (<i>S. foliosa</i>) habitat
Salt marsh harvest mouse (<i>R. raviventris</i>)	% area where $z^* > 1$	Nesting habitat and refuge during extreme events
California clapper rail (<i>R. longirostris obsoletus</i>)	% area where $z^* > 1$	Nesting habitat and refuge during extreme events
	% area where vegetation heights are > 20 cm above MAT	Refuge from predation

forages for food at the marsh edge in sloughs and adjacent mudflats (Eddleman and Conway, 1998). Marsh habitat structure appears to be of greater consequence to patterns of *R. longirostris obsoletus* use than composition (Foin et al., 1997). Vegetation functions primarily as protection from predators and substrate for nesting. Various plant species are used in the construction of nests, but predominant plants include *Grindelia stricta*, *S. foliosa*, and *S. pacifica*. Considerable variability exists in morphologies of these plants, but suitable nesting locations used by the rails have been variously identified as vegetation 0.75 m or higher above the marsh plain (typically in *G. stricta*; De Groot, 1927) and for light-footed clapper rails (*Rallus longirostris levipes*) in Southern California in *S. foliosa* greater than 0.9 m tall (Zedler 1993). Increased risk of nest flooding has been reported when tides at the Golden Gate Bridge are greater than 2 m (Schwarzbach et al., 2006; Zucca, 1954), but the exact tide height that exposes nests to flooding risk is dependent both on the specific site and vegetation features. The area of marsh with vegetation heights exceeding MHHW was used to evaluate the temporal changes in nesting potential at each field site.

Refuge cover from predators of *R. longirostris obsoletus* is of predominant importance during high tides when available habitat is reduced and predator (particularly raptor) hunting efficiency increases (Dekker and Ydenberg, 2004). The normally territorial *R. longirostris obsoletus* will tolerate close contact with neighbors as refuge becomes more limited (C. Overton, personal observation); therefore, only a fraction of available habitat suitable for refuge is needed to support breeding populations. Vegetation needs to be ~20 cm above high water to provide suitable refuge under flood conditions; often this is only available along levee faces, particularly during the winter when *Spartina* spp. senesce and degrade (Callaway and Josselyn, 1998). The current probability density function of maximum vegetation heights within five elevation zones ($z^* < 0$, $0 < z^* < 0.3$, $0.3 < z^* < 0.8$, $0.8 < z^* < 1$, and $1 < z^*$) was super-imposed onto the modeled wetland surface elevation at each time step, and the area projected to have vegetative cover exceeding 20 cm above MHHW was

calculated as potential *R. longirostris obsoletus* refuge. This analysis did not include susceptibility to increased storminess, only vulnerability to tidal action. Current water surface elevations (tide ranges) plus relative SLR were used to explore the inundation patterns of the future marsh surface since the spatial variability and the temporal variability in changes to tide range are unclear at this time.

Results

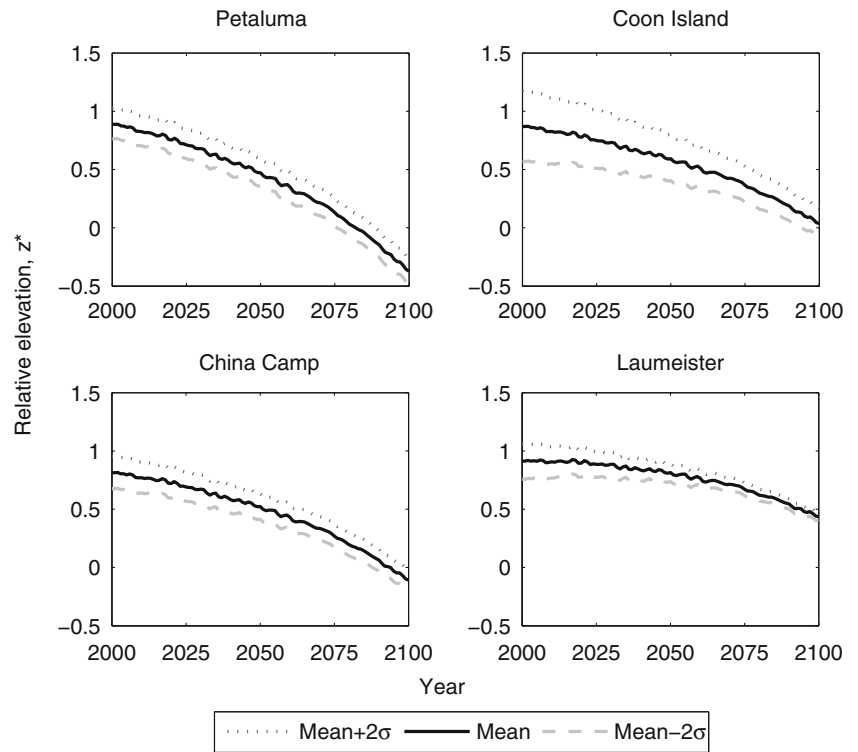
Wetland Elevations and Tidal Ranges

The mean elevation and standard deviation of elevation of each site are presented in Table 3. At all sites, the marsh surface was typically relatively flat and close to the elevation of MHW. Water levels measured by Takekawa et al. (2013) at each field site and tidal datums from VDatum are reported in Table 2. By definition, $z^* = 0$ at MSL and $z^* = 1.0$ at MHHW. Additionally, MHW typically occurs at a z^* of ~0.8 for each field site despite differing absolute elevations of MSL and tide ranges.

Model Results

In all of the scenarios (Fig. 6), marsh elevation decreased by the end of the century and reflected the changes in relative sea level (Fig. 3). Only at Laumeister marsh did elevation remain nearly constant for several decades before decreasing. This lagged response to a temporally variable SLR led to an expansion of low marsh area after 2030, but elevation did not drop below MSL at any time during the Laumeister marsh simulations (Fig. 7). At the other three sites, the simulations of elevation ended at or below MSL ($z^* = 0$). In all of the simulations, the low, mean, and high elevation scenarios began to converge (the relative difference in elevations was smaller at the end of the century than the differences in initial elevations). The nonlinear decrease in simulated wetland elevations corresponds to the shape of the SLR curve used in the simulations.

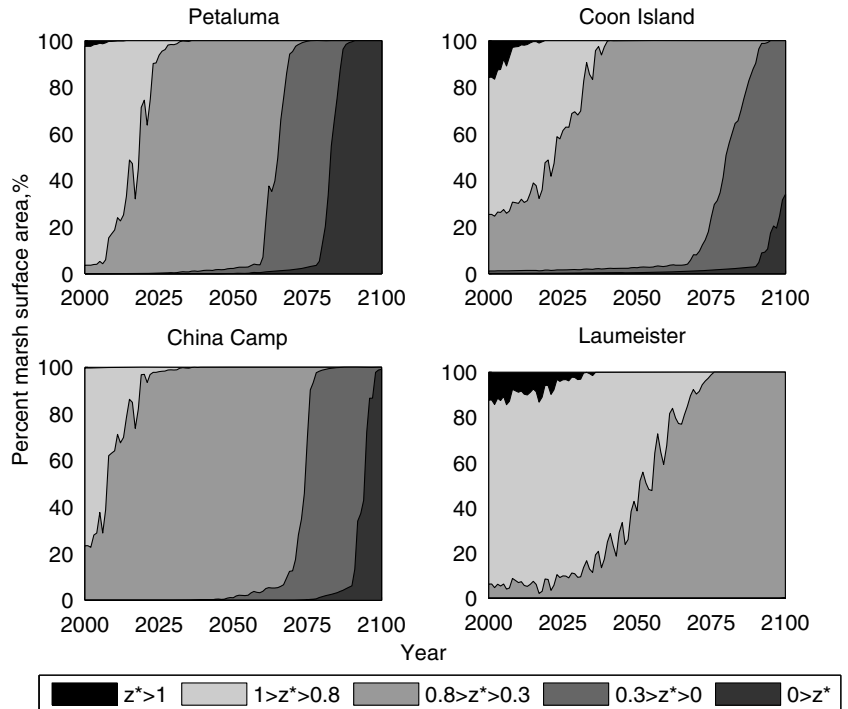
Fig. 6 Modeled scenarios of marsh elevation change for all sites. Dimensionless elevation is plotted versus model year. Low, mean, and high elevations in each scenario are the mean elevation, \bar{z} , and $\bar{z} \pm 2\sigma$. Only the high elevation scenario at each site starts above MHHW, $z^*=1$, and most scenarios finish below MSL, $z^*=0$



At Petaluma marsh and China Camp marsh, the sites with the lowest sediment accumulation rates, large changes in areal distribution of marsh elevation occurred by 2025 and 2075, respectively (Fig. 7). Initially, all high marsh above MHHW was lost, and by 2025, almost all of the marsh area was below MHW. Although $z^*=0.8$ was not defined as a critical habitat

criteria for the species of concern here, there was a significant change in habitat function as the entire marsh surface would be submerged on most high tides at that elevation. By 2075, all marsh area was below $z^*=0.3$, which is the elevation that divides *S. foliosa* and *S. pacifica* habitat. At the end of the simulation, almost all of the marsh area at these two sites was

Fig. 7 Area of marsh surface within a given dimensionless elevation range for all sites for the duration of the simulation period. MHHW occurs at an elevation of $z^*=1$ and MSL at $z^*=0$. MHW occurs at $z^*=0.8$, and the vegetative transition between *S. pacifica* and *S. foliosa* occurs at $z^*=0.3$



below MSL. A similar pattern was observed at Coon Island marsh though the changes in elevation were not as large and the distribution of marsh elevations lagged behind those simulated for China Camp and Petaluma marshes. The Laumeister marsh simulation was the only one that did not forecast an initial decrease in marsh elevation and loss of area with elevations above MHHW in the first few decades of the century, but all marsh area above $z^*=1$ was lost by 2050.

Model Performance Test

For the steady, historic SLR runs, WARMER recreated the soil core profile for bulk density very well and, while underestimating organic matter content at all but Laumeister marsh, captured the trend of decreasing organic matter with increasing depth through the soil profile (Figure SM1, Supplemental Materials). The calculated equilibrium elevations of all four salt marshes fall within the colonization elevations of *S. foliosa* and *S. pacifica* described by Atwater and Hedel (1976), though the equilibrium elevation at Petaluma marsh falls well below the observed and expected equilibrium elevation for *S. pacifica*-dominated marshes near MHW (Table 6). For three of the four sites, the equilibrium elevation for the given accumulation functions and recent SLR is between MHW and MAT. China Camp and Coon Island marshes have measured median elevations very close to the calculated equilibrium elevation. The equilibrium elevation at Laumeister marsh is between MHHW and MAT. This site in South San Francisco Bay may have experienced a higher relative SLR due to groundwater-extraction-induced subsidence (Poland and Ireland, 1988), and the measured accumulation rate may reflect the more rapid filling of the accommodation space generated by subsidence and SLR rather than a quasi-equilibrium with SLR at the mouth of the bay. The equilibrium elevation of Petaluma marsh is below MSL, but within the colonization elevation of *S. foliosa* reported by Atwater and Hedel (1976). Model performance for Petaluma marsh will be addressed more fully in the discussion.

The constant rate of SLR applied during the spin-up period varied for each of the 12 model scenarios in order to steadily

maintain the desired initial elevation for the 200-year spin-up. Comparison of these SLR values to the measured rate of SLR provides an additional test of model performance. SLR during the spin-up period ranged from 0.4–5.9 mm/year, but the mean for mid and high marsh scenarios, with initial elevations \geq MHW, was 2.1 mm/year. Coon Island and China Camp marshes required an SLR most similar to the measured historic rate. Low marsh elevations required a mean SLR rate of 4 mm/year during the spin-up period.

Sensitivity Analysis

The sensitivity analysis of WARMER shows that the greatest differences in final elevation occurred when SLR and inorganic sediment accumulation were varied (Fig. 8). On average, the scenarios with the largest sediment accumulation were able to keep pace with SLR. Scenarios with only 50 cm of SLR by the end of the century had an average increase in elevation of 7 %. The small variations in porosity that were observed in the marsh sediment cores did not lead to large changes in final elevation despite the strong nonlinearity between porosity and volume. The influence of organic matter accumulation was also small (<2 % change in final mean elevation) despite the observed range of accumulation rates varying by ± 50 % from the mean. Initial elevation also did not have a large impact on final elevation. However, the scenarios with the lowest sediment accumulation rate did have a larger dependence on initial elevation than the other accumulation rate scenarios. The negative feedback between elevation and sediment accumulation was strong enough to mitigate this influence in the mean and high sediment input scenarios.

Habitat Evaluation

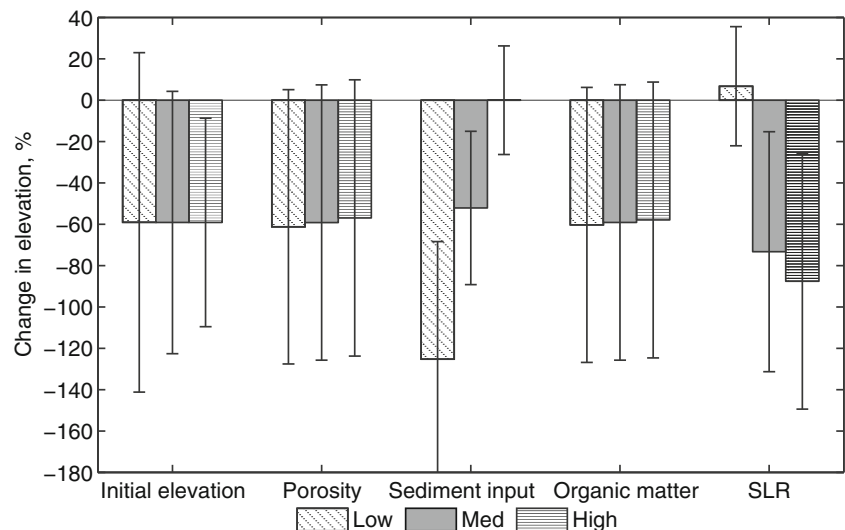
Vegetation

Vegetative habitat was evaluated based on the elevation ranges of the dominant plant species: $0 < z^* < 0.3$ for *S. foliosa* and $0.3 < z^*$ for *S. pacifica*. Initially, *S. foliosa* was present at the fringes of the marsh edge and along channel banks where the

Table 6 Model performance test metrics. Equilibrium elevation reported as elevation relative to MSL and z^* for each site when the model is run with an SLR equal to the historic rate of SLR in San Francisco Bay. The SLR required to maintain each initial elevation during the spin-up period is also reported

Site	Equilibrium elevation for 2.01 mm/year SLR		SLR required for spin-up period (mm/year)		
	(cm)	z^*	Low elevation	Mean elevation	High elevation
China Camp	75.1	0.8	2.6	2.0	1.4
Petaluma	-10.1	-0.12	0.8	0.6	0.4
Laumeister	117.8	1.29	7.9	5.9	4.2
Coon Island	78.6	0.9	4.7	2.3	0.4

Fig. 8 Results of the sensitivity analysis. Each bar is the mean percent change in elevation for 81 runs with the indicated parameter. Error bars indicate ± 1 standard deviation from the mean. Inputs for the sensitivity analysis scenarios are provided in Table 4



marsh surface is lower, which was only 1–1.2 % of the marsh surface in all scenarios. As elevation decreased in the scenarios for China Camp, Petaluma, and Coon Island marshes, the area of marsh in the *S. foliosa* elevation range slowly expanded over the first half of the simulation period and then rapidly with the entire area of the marsh plain below MSL by the end of the simulation period. At Laumeister marsh, the marsh plain was uniformly above $z^*=0$ for the entire simulation period with an expansion of the *S. foliosa* elevation zone and corresponding loss of the *S. pacifica* zone after 2030.

Salt Marsh Harvest Mouse and California Clapper Rail

Just 0.4 and 2.5 % of China Camp marsh and Petaluma marsh, respectively, were initially above the critical marsh plain elevation of $z^*=1$, MHHW, while 16 and 13 % of the marsh plain at Coon Island and Laumeister marshes provided effective habitat for nesting and refuge for *R. raviventris* and *R. longirostris obsoletus*. At China Camp, Petaluma, and Coon Island marshes, this effective high marsh habitat was gone after two decades. Very little of the 15 % of Laumeister marsh habitat above $z^*=1$ was lost before 2030; however, a decrease in relative elevation of the marsh plain led to complete loss of this habitat by 2050.

Vegetative cover for avian refuge where vegetation heights exceed MHHW by at least 20 cm was calculated to provide effective habitat over 80–90 % of the marsh at the beginning of all scenarios (Fig. 9). This metric of available refugia generally decreased with decreasing elevation, and no refuge remained by the end of the simulations at Petaluma and China Camp marshes. Only 20 % of the marsh refuge remained at Coon Island marsh by the end of the period. There was a marginal increase in available habitat when the marsh surface elevations dropped below $z^*=0.3$ towards the end of the simulation period because *S. foliosa* is generally several decimeters taller than *S. pacifica* (vegetation heights are typically 40–60 cm for

$z^*>0.3$ and 100–180 cm for $z^*<0.3$). However, the gain in refuge habitat was rapidly lost as the marsh plain continued to lose elevation relative to sea level. Laumeister marsh experienced only a small increase in vegetative refuge habitat over the first half of the simulation period. Available habitat decreased in the second half of the simulation period as more of the marsh surface was projected to be below MHHW ($z^*=0.8$).

Discussion

The model scenarios showed that all four of the salt marsh sites in the San Francisco Estuary are likely to experience significant elevation decreases on decadal timescales (Fig. 6). The decreases in elevation occurred early in the model scenarios at China Camp and Petaluma, the marshes with the lowest organic matter and sediment accumulation rates. The

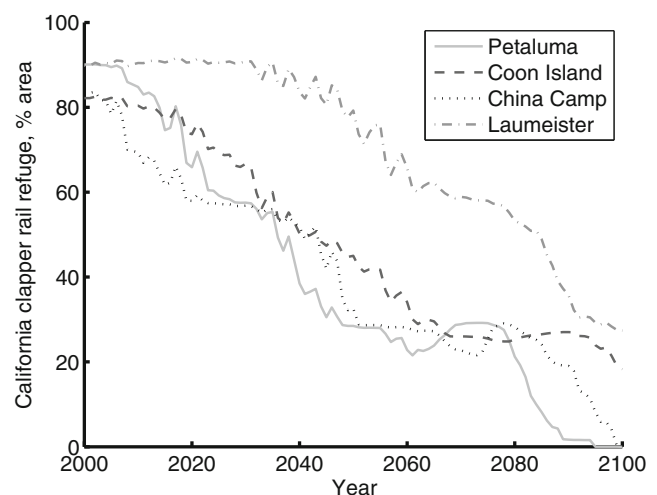


Fig. 9 *R. longirostris obsoletus* habitat availability at MHHW. Projected marsh area (%) where elevation plus maximum vegetation height exceeds MHHW by at least 20 cm

100-year scenario ended with the entire marsh plain below MSL for both of these marshes (Fig. 7). Changes in elevation at Coon Island marsh were similar to those at China Camp and Petaluma marshes, but occurred slightly later in the scenarios and less than 40 % of the modeled marsh surface was below MSL at the end of the simulation period (Fig. 7). Laumeister marsh, the site with the greatest accumulation rates, had little change in relative elevation during the first half of the simulation period before degrading when SLR accelerated towards the second half of the century.

Similar to Kirwan et al. (2010), the sites with greater sediment supply were initially able to keep up with changes in sea level, but even these marshes were not able to keep pace with SLR by the end of the century. Stralberg et al. (2011) also found that the San Francisco Estuary marshes with the lowest sediment supply were the most vulnerable to drowning. In their paper, Petaluma marsh was in a high sediment subregion, whereas in this study, Petaluma had the lowest calibrated accumulation curve for sediment. Petaluma marsh is in an area generally considered to have a very high suspended-sediment supply (Schoellhamer et al., 2007), but there is no research showing how much of this sediment actually deposits on the marsh plain. Sediment delivery in Stralberg et al. (2011) was based on SSC in San Pablo Bay, and this study may have underestimated the amount of inorganic sedimentation at Petaluma marsh. Another possibility is that the sediment cores used to calibrate the sediment input function for WARMER had mean inorganic sedimentation rates that were lower than the actual inorganic sedimentation for the marsh. This is an example of how important accurate parameterization of the elevation-dependent sediment input function is to assessing marsh sustainability. Modeled sediment accumulation could be improved through direct measurement of sediment accumulation across a greater elevation range within the intertidal zone in San Francisco Estuary and by improving the SSC estimates and sediment flux calculation for concentration-driven models like Stralberg et al. (2011).

It is important to note that uncertainty in the input parameters could be large and the corresponding uncertainty in marsh elevation increases with time in these scenarios, but the sensitivity analysis provides an evaluation of a range of possible model inputs and defines the range of values that are likely to lead to marsh survival. The sensitivity analysis of WARMER showed that the magnitudes of the sediment input function and SLR were the two most sensitive parameters. Only the scenarios with the highest sediment input rate and the lowest SLR were able to aggrade sufficiently to offset SLR. This result was also found for the scenarios run by Stralberg et al. (2011). Like the Krone (1987) model, WARMER reflects the shape of the SLR curve. In addition, the results demonstrated that not only is the magnitude of SLR over the next century important, but the acceleration of SLR in the latter half of the century is also critical to marsh sustainability and habitat response (Fig. 6).

Callaway et al. (1996) and Deverel et al. (2008) found that initial elevation and porosity were sensitive inputs for the Callaway model. The range of observed porosities observed in the sediment cores did not greatly impact the change in elevation in the scenarios despite the strongly nonlinear relationship between porosity and soil volume. Initial elevation also did not have a large impact on the magnitude of change, although it should be noted that initial elevation was a moderately sensitive parameter in the sensitivity analysis for the scenarios with the lowest sediment accumulation rates. The strength of the stabilizing feedback between elevation and sediment accumulation was not strong enough to erase the impact of the initial condition over the course of the simulation period. It is likely that relative sensitivity of these terms would increase for lower rates of sediment accumulation and SLR in WARMER, but the much larger magnitude of sediment accumulation and SLR terms observed and predicted for the San Francisco Estuary scenarios overwhelmed the impact of initial elevation and porosity.

The elevation of marshes in the San Francisco Estuary dominated by *S. pacifica* does not appear to be greatly influenced by organic matter production. The magnitude of organic matter accumulation rates calculated from marsh sediment cores was much smaller than the magnitude of productivity defined by Morris et al. (2002) for *S. alterniflora* meadows and an order of magnitude smaller than the measured inorganic sediment accumulation rates. However, this may be a finding specific to *S. pacifica*, which is not as productive as *S. alterniflora*, and therefore would have to be re-tested further upstream in the San Francisco Estuary where brackish marshes and tidal freshwater marshes are dominated by high productivity vegetation such as cattails (*Typha* spp.) and bulrushes (*Schoenoplectus* spp.). Drexler et al. (2009) and Deverel et al. (2008) showed that organic matter accumulation rates in Delta peats were more than four times greater than the highest rate of organic matter accumulation measured in the San Francisco salt marsh sediment cores used to calibrate WARMER.

Site-specific data were essential for calibrating the marsh accretion model. For example, inorganic sediment accumulation rates, the most sensitive model parameter, varied by more than an order of magnitude between the four salt marshes of this study. Additional species-specific organic matter productivity data to better define above- and belowground organic matter accumulation functions could also improve and refine WARMER as well as other marsh elevation models being applied in San Francisco Estuary.

Performance tests demonstrate that the model generally predicts equilibrium elevations within the colonization elevation of marsh vegetation and within a few centimeters of measured median marsh elevations at China Camp and Coon Island marshes (Table 6). Calculated equilibrium marsh elevations deviate the most from current measured marsh elevations where subsidence may have caused a local deviation for the regional SLR (Laumeister marsh) trend or where accumulation

rates may not be well defined by the sediment cores (Petaluma marsh). Because sediment accumulation at Petaluma appears to be unrealistically low, those marsh scenarios are probably more representative of what would happen if sediment supply were drastically reduced to a presently healthy, high marsh. Such a reduction could be caused by anthropogenic changes to the marsh plain or continuation of presently decreasing sediment supply (Wright and Schoellhamer, 2004; Cloern et al., 2011; Schoellhamer, 2011). Additionally, SLR rates used for the spin-up periods indicate that high marsh, above MHW, is generally a stable landscape feature for the given historic rate of SLR and measured accumulation rates. However, for the given model parameters and historic rate of SLR, low marsh is either a transitory feature or requires the inclusion of processes such as erosion or wave action to counteract the negative feedback of increasing accumulation with increased inundation that are generally not included in 1-D marsh accretion models.

The scenarios showed a decrease in vegetative habitat, especially *S. pacifica*, by the end of the century. There is potential for an expansion of the habitat for *S. foliosa* (as well as *S. alterniflora* and its hybrids), but this is uncertain because the vegetative response of a drowning marsh has not been well documented. The marsh may drown too quickly for *S. foliosa* to colonize the marsh plain as the elevations decrease below $z^*=0.3$. Additionally, the vegetative responses of both *S. pacifica* and *S. foliosa* are not well constrained. It is unclear whether the vegetation will respond to increased atmospheric CO₂ by increasing productivity and thereby offsetting degradation of the marsh plain elevation by SLR (Langley et al., 2009). The negative feedback between organic productivity and increased flooding associated with SLR noted by Kirwan and Guntenspergen (2012) is not fully captured by the organic matter input function in WARMER, nor does the model adaptation reflect the observed differences in above- and belowground organic matter productivity that might provide a stabilizing mechanism for high marshes (Kirwan and Guntenspergen, 2012). Vegetative marsh accretion processes in Pacific tidal wetlands, specifically in *S. pacifica*, would be worthy of further investigation to fully capture the feedback between organic matter productivity and inundation.

The area of effective habitat of elevation above $z^*=1$ for *R. raviventris* and *R. longirostris obsoletus* decreased rapidly with decreasing marsh plain elevation at Petaluma, China Camp, and Coon Island marshes. Laumeister marsh area above $z^*=1$ remained nearly constant for the first 30 years of the simulation period, but that habitat was eventually lost. At China Camp marsh, only the footprint of the current marsh was modeled, and the model domain did not include the adjacent uplands that could provide future high marsh habitat if the marsh transgresses as sea level rises. Similarly, only a portion of Petaluma marsh was modeled, and adjacent areas could provide future high marsh habitat. Coon Island and Laumeister marshes are more isolated, and lateral marsh

transgression is less likely at these sites. Because WARMER is a 1-D vertical accretion model extrapolated over the marsh surface, the simulations do not incorporate wave erosion at the marsh edge or channel migration. A process-based marsh-morphology model would be capable of providing improved projections of future areal marsh elevations (e.g., Fagherazzi et al., 2012). However, the processes not included in WARMER are largely processes that degrade elevation, and the projections of elevation change across the marsh surface may, therefore, provide an estimate of a best case scenario.

Vegetative cover that provides critical avian refuge was significantly degraded at all sites, except for Laumeister marsh, within the first three decades of the scenarios. Because *S. foliosa* is taller than *S. pacifica*, there was a small increase in vegetative refuge when the marsh plain dropped below $z^*=0.3$, but the small gain in vegetative cover was rapidly lost due to decreasing marsh plain elevation. The area with vegetative cover for *R. longirostris obsoletus* was greater than the area of marsh plain above $z^*=1$, indicating that there may be viable *R. longirostris obsoletus* habitat later in the scenarios despite relative lowering of marsh plain elevations. This difference in results based on the *R. longirostris obsoletus* habitat metrics for marsh plain elevation and vegetation elevation relative to MHHW emphasizes the need to develop and improve species-specific habitat metrics in addition to evaluating the evolution of marsh plain elevation. The implication of WARMER scenarios based on a moderate 125-cm SLR is that the habitat for *R. longirostris obsoletus* is likely to have a severe reduction by 2100. The use of z^* , the nondimensional elevation, to present results and habitat metrics provides a format that was easily comparable across all sites and allowed for the use of a single habitat metric where absolute elevations and tide ranges differ.

Acknowledgments We would like to thank the U.S. Geological Survey Western Ecological Research Center and the U.S. Geological Survey National Climate Change Wildlife Science Center for providing financial support. Additional support was provided by the U.S. Geological Survey Priority Ecosystem Science Program and the Computational Assessments of Scenarios of Change for the Delta Ecosystem (CASCaDE II) project. CASCaDE II is supported by a grant from the Delta Science Program. Any opinions, findings, and conclusions or recommendations expressed in this material are those of the authors and do not necessarily reflect the views of the Delta Science Program. This is CASCaDE report #42. Kevin Buffington, Kyle Spragens, Christopher Fuller, and Evyan Borgnis provided valuable guidance and information for the development of this project. Glenn Guntenspergen, Donald Cahoon, Lisa-Marie Wyndham-Myers, and two anonymous referees provided thoughtful reviews that contributed to the improvement of the manuscript. We would like to thank the managers of the San Francisco Bay National Wildlife Refuges, East Bay Regional Parks, Department of Fish and Wildlife Napa-Sonoma Marshes, and China Camp State Park and National Estuarine Research Reserve for permission and logistical support. The use of trade names is for descriptive purposes only and does not imply government endorsement.

References

- Allen, J.R.L. 1995. Salt-marsh growth and fluctuating sea level: implications of a simulation model for Flandrian coastal stratigraphy and peat-based sea level curves. *Sedimentary Geology* 100: 21–45.
- Bias, M.A. and M.L. Morrison. 1999. Movements and home range of salt marsh harvest mice. *The Southwestern Naturalist* 44(3): 348–353.
- Bias, M.A. and M.L. Morrison. 2006. Habitat selection of the salt marsh harvest mouse and sympatric rodent species. *The Journal of Wildlife Management* 70(3): 732–742.
- Bindoff, N.L., J. Willebrand, V. Artale, A. Cazenave, J. Gregory, S. Gulev, K. Hanawa, C. Le Quéré, S. Levitus, Y. Nojiri, C.K. Shum, L.D. Talley, and A. Unnikrishnan. 2007. Observations: oceanic climate change and sea level. In *Climate change 2007: the physical science basis. Contribution of Working Group I to the Fourth Assessment Report of the Intergovernmental Panel on Climate Change*, ed. S. Solomon, D. Qin, M. Manning, Z. Chen, M. Marquis, K.B. Averyt, M. Tignor, and H.L. Miller. New York: Cambridge University Press.
- Bricker-Urso, S., S.W. Nixon, J.K. Cochran, D.J. Hirschberg, and C. Hunt. 1989. Accretion rates and sediment accumulation in Rhode Island marshes. *Estuaries* 12: 300–317.
- Cahoon, D.R., D.J. Reed, and J.W. Day Jr. 1995. Estimating shallow subsidence in microtidal salt marshes of the southeastern United States: Kaye and Barghoorn revisited. *Marine Geology* 128: 1–9.
- Callaway, J.C., and M.N. Josselyn. 1998. The introduction and spread of smooth cordgrass (*Spartina alterniflora*) in South San Francisco Bay. *Estuaries* 15: 218–226.
- Callaway, J., J.A. Nyman, and R.D. DeLaune. 1996. Sediment accretion in coastal wetlands: a review and simulation model of processes. *Current Topics in Wetland Biogeochemistry* 2: 2–23.
- Callaway, J.C., E.L. Borgnis, R.E. Turner, and C.S. Milan. 2012. Carbon sequestration and sediment accretion in San Francisco Bay tidal wetlands. *Estuaries and Coasts* 35: 1163–1181.
- Cayan, D., Tyree, M., Dettinger, M., Hidalgo, H., Das, T., Maurer, E., Bromirski, P., Graham, N. and Flick, R., 2009. Climate change scenarios and sea-level rise estimates for the California 2008 climate change scenarios assessment. California Climate Change Center. CEC-500-2009-014-D, 62 pp.
- Cloern, J.E., N. Knowles, L.R. Brown, D. Cayan, and M.D. Dettinger. 2011. Projected evolution of California's San Francisco Bay-Delta-River System in a century of climate change. *PLoS ONE* 6(9): e24465.
- Curcó, A., C. Ibañez, J.W. Day, and N. Prat. 2002. Net primary production and decomposition of salt marshes of the Ebre Delta (Catalonia, Spain). *Estuaries* 25: 309–324.
- D'Alpaos, A. 2011. The mutual influence of biotic and abiotic components on the long-term geomorphodynamic evolution of salt-marsh ecosystems. *Geomorphology* 126: 269–278.
- D'Alpaos, A., S. Lanzoni, M. Marani, and A. Rinaldo. 2007. Landscape evolution in tidal embayments: modeling the interplay of erosion, sedimentation, and vegetation dynamics. *Journal of Geophysical Research*. 112, F01008.
- Day Jr., J.W., and P.H. Templet. 1989. Consequences of sea level rise: implications from the Mississippi delta. *Coastal Management* 17: 241–257.
- Day Jr., J.W., J. Rybczyk, F. Scarton, A. Rismondo, D. Are, and G. Cecconi. 1999. Soil accretionary dynamics, sea-level rise and the survival of wetlands in Venice Lagoon: a field and modelling approach. *Estuarine Coastal and Shelf Science* 49: 607–628.
- De Groot, D.S. 1927. The California clapper rail: its nesting habits, enemies and habitat. *The Condor* 29: 259–270.
- Dekker, D., and R. Ydenberg. 2004. Raptor predation on wintering dunlins in relation to the tidal cycle. *The Condor* 106: 415–419.
- Deverel, S.J., J.Z. Drexler, T. Ingram, and C. Hart. 2008. *Simulated Holocene, recent, and future accretion in channel marsh islands and impounded marshes for subsidence mitigation, Sacramento–San Joaquin Delta*. California, USA: REPEAT Project Final Report to the CALFED Science Program of the Resources Agency of California. 60 pp.
- Drexler, J.Z. 2011. Peat formation processes through the millennia in tidal marshes of the Sacramento–San Joaquin Delta, California, USA. *Estuaries and Coasts* 34: 900–911.
- Drexler, J.Z., C.S. de Fontaine, and T.A. Brown. 2009. Peat accretion histories during the past 6,000 years in marshes in the Sacramento–San Joaquin Delta, California, USA. *Estuaries and Coasts* 32: 871–892.
- Eddleman, W.R., and C.J. Conway. 1998. Clapper rail (*Rallus longirostris*). In *The birds of North America*, no. 240, ed. A. Poole and E. Gill. Philadelphia, PA, USA: The birds of North America. Inc.
- Erwin, R. M., Sanders, G.M., Prosser, D.J., and Cahoon, D.R., 2006. High tides and rising seas: potential effects on estuarine waterbirds. In: *Vertebrates of tidal marshes: ecology, evolution and conservation*. Studies in avian biology, eds. R. Greenberg, S. Droege, J. Maldonado, and M. V. McDonald, Lawrence, KS: Allen Press.
- Euliss Jr., N.H., L.M. Smith, D.A. Wilcox, and B.A. Browne. 2008. Linking ecological processes with wetland management goals: charting a course for a sustainable future. *Wetlands* 28: 553–562.
- Faber, P. 2000. Grass wars: good intentions gone awry. Why would anyone bring an alien cordgrass into S. F. Bay? *California Coast and Ocean* 16: 14–17.
- Fagherazzi, S., M.L. Kirwan, S.M. Mudd, G.R. Guntenspergen, S. Temmerman, A. D'Alpaos, J. van de Koppel, J. Rybczyk, E. Reyes, C. Craft, and J. Clough. 2012. Numerical models of salt marsh evolution: ecological, geomorphic, and climatic factors. *Reviews of Geophysics* 50, RG1002.
- Fisler, G.F. 1963. Effects of salt water on food and water consumption and weight of harvest mice. *Ecology* 44(3): 604–608.
- Fisler, G.F. 1965. Adaptations and speciation in harvest mice of the marshes of San Francisco Bay. *University of California Publications in Zoology* 77: 1–108.
- FitzGerald, D.M., M.S. Fenster, B.A. Argow, and I.V. Buynevich. 2008. Coastal impacts due to sea-level rise. *Annual Review of Earth and Planetary Sciences* 36: 601–647.
- Foin, T.C., E.J. Garcia, R.E. Gill, Culbertson, and J.N. Collins. 1997. Recovery strategies for the California clapper rail (*Rallus longirostris obsoletus*) in the heavily-urbanized San Francisco estuarine ecosystem. *Landscape and Urban Planning* 38: 229–243.
- French, J.R. 1993. Numerical simulations of vertical marsh growth and adjustment to accelerated sea-level rise, North Norfolk, UK. *Earth Surface Processes and Landforms* 18: 63–81.
- French, J.R. 2006. Tidal marsh sedimentation and resilience to environmental change: exploratory modeling of tidal, sea-level and sediment supply forcing in predominantly allochthonous systems. *Marine Geology* 235: 119–136.
- Hatton, R.S., R.D. DeLaune, and W.H. Patrick Jr. 1983. Sedimentation, accretion and subsidence in marshes of Barataria Basin, Louisiana. *Limnology and Oceanography* 25: 494–502.
- Hogle, I., and Olofson Environmental Incorporated, 2011. San Francisco Estuary invasive *Spartina* project monitoring report for 2010.
- Hulst, M.D., L.S. Hall, M.L. Morrison and M.L. Balis. 2001. Assessing salt marsh harvest mouse movements during high tides, San Pablo Bay, California. *Transactions of the Western Section of the Wildlife Society* 37: 88–91.
- Kirwan, M.L., and G.R. Guntenspergen. 2012. Feedbacks between inundation, root production, and shoot growth in a rapidly submerging brackish marsh. *Journal of Ecology*. doi:10.1111/j.1365-2745.2012.
- Kirwan, M.L., and A.B. Murray. 2007. A coupled geomorphic and ecological model of tidal marsh evolution. *Proceedings of the National Academy of Science* 104: 6118–6122.
- Kirwan, M.L., G.R. Guntenspergen, and J.T. Morris. 2009. Latitudinal trends in *Spartina alterniflora* productivity and the response of

- coastal marshes to global change. *Global Change Biology* 15: 1982–1989.
- Kirwan, M.L., G.R. Guntenspergen, A. D'Alpaos, J.T. Morris, S.M. Mudd, and S. Temmerman. 2010. Limits on the adaptability of coastal marshes to rising sea level. *Geophysical Research Letters* 37, L23401.
- Krone, R.B., 1987. A method for simulating historic marsh elevations. *Coastal Sediments 1987*, ASCE, New Orleans. 317–323.
- Langley, J.A., K.L. McKee, D.R. Cahoon, J.A. Cherry, and J.P. Megonigal. 2009. Elevated CO₂ stimulates marsh elevation gain, counterbalancing sea-level rise. *Proceedings of the National Academy of Sciences* 106(15): 6182–6186.
- Mitsch, W.J., and J.G. Gosselink. 2000. *Wetlands*, 3rd ed. New York: John Wiley & Sons.
- Morris, J.T., P.V. Sundareshwar, C.T. Nietch, B. Kjerfve, and D.R. Cahoon. 2002. Response of coastal wetlands to rising sea level. *Ecology* 83: 2869–2877.
- Mudd, S.M., S.M. Howell, and J.T. Morris. 2009. Impact of dynamic feedbacks between sedimentation, sea-level rise, and biomass production on near-surface marsh stratigraphy and carbon accumulation. *Estuarine Coastal and Shelf Science* 82: 377–389.
- Nicholls, R.J., F.M.J. Hoozemans, and M. Marchand. 1999. Increasing flood risk and wetland losses due to global sea-level rise: regional and global analyses. *Global Environmental Change* 9(SUPPL): S69–S87. 9.
- Poland, J.F., and Ireland, R.L., 1988. Land subsidence in the Santa Clara Valley, California, as of 1982: U.S. Geological Survey Professional Paper 497-F, 61 p. <http://pubs.er.usgs.gov/publication/pp497F>
- Ruhl, C.A., and D.H. Schoellhamer. 2004. Spatial and temporal variability of suspended-sediment concentration in a shallow estuarine environment. *San Francisco Estuary and Watershed Science* 2: 1.
- Rybczyk, J.M., and D.R. Cahoon. 2002. Estimating the potential for submergence for two wetlands in the Mississippi River delta. *Estuaries* 25(5): 985–998.
- Scarton, F., J.W. Day, and A. Rismondo. 2002. Primary production and decomposition of *Sarcocornia fruticosa* (L.) Scott and *Phragmites australis* Trin. Ex Steudel in the Po Delta, Italy. *Estuaries* 25: 325–336.
- Schoellhamer, D.H. 1996. Factors affecting suspended-solids concentrations in South San Francisco Bay, California. *Journal of Geophysical Research* 101: 12,087–12,095.
- Schoellhamer, D.H. 2002. Variability of suspended-sediment concentration at tidal to annual time scales in San Francisco Bay, USA. *Continental Shelf Research* 22: 1857–1866.
- Schoellhamer, D.H. 2011. Sudden clearing of estuarine waters upon crossing the threshold from transport–to supply–regulation of sediment transport as an erodible sediment pool is depleted: San Francisco Bay, 1999. *Estuaries and Coasts* 34: 885–899.
- Schoellhamer, D.H., T.E. Mumley, and J.E. Leatherbarrow. 2007. Suspended sediment and sediment-associated contaminants in San Francisco Bay. *Environmental Research* 105(1): 119–131.
- Schwarzbach, S.E., J.D. Albertson, and C.M. Thomas. 2006. Effects of predation, flooding, and contamination on reproductive success of California clapper rails (*Rallus longirostris obsoletus*) in San Francisco Bay. *The Auk* 123: 45–60.
- Shellhammer, H.S. 1982. *Reithrodontomys raviventris*. *Mammalian Species* 169: 1–3.
- Stralberg, D., M. Brennan, J.C. Callaway, J.K. Wood, L.M. Schile, D. Jongsomjit, M. Kelly, V.T. Parker, and S. Crooks. 2011. Prospects for tidal marsh sustainability in San Francisco Bay: spatial habitat scenarios and sensitivity analysis. *PLoS ONE* 6(11): e27388.
- Takekawa, J.Y., K.M. Thorne, K.J. Buffington, K.A. Spragens, K.M. Swanson, J.Z. Drexler, D.H. Schoellhamer, C.T. Overton, and M.L. Casazza. 2013. Final report for sea-level rise response modeling for San Francisco Bay estuary tidal marshes. U.S. Geological Survey Open File Report 2013–1081, 161 p.
- Van de Pol, M., Y. Vindened, and B.E. Saether. 2010. Effects of climate change and variability on population dynamics in a long-lived shorebird. *Ecology* 91: 1192–1204.
- Wright, S.A., and D.H. Schoellhamer. 2004. Trends in the sediment yield of the Sacramento River, California, 1957–2001. *San Francisco Estuary and Watershed Science*. 2(2), article 2.
- Xu, J., Myers, E.P., and White, S.A., 2010. VDatum for the coastal waters of North/Central California, Oregon and Western Washington: tidal datums and sea surface topography. NOAA Technical Memorandum NOS CS 22.
- Zedler, J.B. 1993. Canopy architecture of natural and planted cordgrass marshes: selecting habitat evaluation criteria. *Ecological Applications* 3: 123–138.
- Zervas, C., 2009. Sea level variations of the United States 1854–2006, NOAA Technical Report NOS CO-OPS 053, NOAA National Ocean Service Center for Operational Oceanographic Products and Services, 78 pp.
- Zucca, J.J. 1954. A study of the California clapper rail. *Wasmann Journal of Biology* 13: 135–153.